







DRAFT VERSION JUNE 24, 2022

Typeset using L^AT_EX **modern** style in AAS_TE_X631

paired: A Statistical Framework for Determining Stellar Binarity with *Gaia* RVs. I. Planet Hosting Binaries

QUADRY CHANCE ^{1,2} DANIEL FOREMAN-MACKEY ² SARAH BALLARD ¹
ANDREW R. CASEY ^{3,4} TREVOR J. DAVID ² AND
ADRIAN M. PRICE-WHELAN ²

¹*Department of Astronomy, University of Florida, 211 Bryant Space Science Center, Gainesville, FL, 32611, USA*

²*Center for Computational Astrophysics, Flatiron Institute, Simons Foundation, 162 5th Ave, New York, NY 11238*

³*School of Physics & Astronomy, Monash University, Victoria, Australia*

⁴*Center of Excellence for Astrophysics in Three Dimensions (ASTRO-3D), Australia*

Submitted to ApJ

ABSTRACT

The effect of stellar multiplicity on the formation and evolution of planetary systems is complex. At a demographic level, campaigns with both high-resolution imaging and radial velocity observations indicate that planet formation is strongly disrupted by close binaries, while being relatively unaffected by wide companions. However, the magnitude and distance-limited nature of those tools mean that large ranges of mass ratios and separations remain largely unexplored. The Early Data Release 3 (EDR3) from the *Gaia* Mission includes radial velocity measurements of over 6.5 million targets, which we employ to explore the effect of binary companions within a statistical framework called **paired**. These companions present as a source of excess radial velocity noise in the *Gaia* catalog, when compared to the typical noise for stars of similar spectral type and magnitude. Within this framework, we examine the evidence for stellar multiplicity among the stars surveyed by *NASA*'s *Kepler* and *TESS* missions. We use radial velocity errors published in *Gaia* EDR3 to estimate the probability of an unresolved stellar companion for a large subset of the *Kepler* and *TESS* Input Catalog stars, where possible benchmarking our inferred radial velocity semi-amplitudes against the those from ground-based radial velocity surveys. We determine that we are typically sensitive out to several AU and mass ratios > 0.1 , dependent upon the stellar magnitude. We aim for **paired** to be a useful community tool for the exploration of the effects of binarity on planets at a population level, and for efficient identification of false-positive transit candidates.

Corresponding author: Quadry Chance

qchance@ufl.edu

Keywords: Binary stars (154), Close binary stars (254), Spectroscopic binary stars (1557), Planet hosting stars (1242), Exoplanet astronomy (486), Astrostatistics tools (1887), Astrostatistics (1882)

1. INTRODUCTION

The rapid growth in the number of known exoplanets has enabled subsequent detailed studies of planetary demographics. Investigations of the key relationship between stellar properties and planet occurrence emerged within a decade of the discovery of the first planet around a main-sequence star (e.g. [Fischer & Valenti 2005](#)). The addition of thousands more planets to the known sample has allowed exoplanetary astronomers to map this relationship with increasing detail. The knowledge that planets exist in binaries followed only a year after the discovery that planets reside around other main-sequence stars: the fourth detected exoplanet orbits the K dwarf member of the binary pair 55 Cnc A and B. Twenty years after the first detection of a planet orbiting a single member of a binary, the discovery of Kepler-16b showed that some planets even orbit *both* members. Circumbinary planets and planets in close S-type systems alone now number in the dozens. About half of the FGK stars in the Milky Way have main-sequence companions ([Offner et al. 2022](#)), making this question a critical one for the theory of planet formation.

Previous studies with both adaptive optics imaging (AO) and radial velocity (RV) campaigns have established that binarity plays an important role in shaping planetary systems e.g. ([Holman & Wiegert 1999](#); [Paardekooper et al. 2008](#); [Marzari & Gallina 2016](#); [Kraus et al. 2012](#); [Su et al. 2021](#)). [Wang et al. \(2014\)](#) showed that planet occurrence drops to a third for stars with companions at separations of 100 AU, when compared to single stars. This figure drops to a tenth for stars with companions at 10 AU. Indeed, [Moe & Kratter \(2021\)](#) showed that all but 15% of planetary systems are suppressed due to the presence of companion stars interior to 10 AU. [Ziegler et al. \(2021\)](#) found that suppression at the 15% survival level holds for separations as wide as 50 AU. With an adaptive optics imaging campaign sensitive to larger separations, [Kraus et al. \(2016\)](#) found that 30% of planetary systems survive, when the host star has a companion interior to 50 AU (relative to stars without a companion). This suppression effect, per [Moe & Kratter \(2021\)](#) seems to weaken or disappear at “wide” separations of > 200 AU.

The physical mechanism responsible for the effect of binarity on the formation of planets may occur at the disk stage, in some cases entirely preventing that disk from forming ([Silsbee & Rafikov 2015](#)). The literature on the impact of stellar multiplicity upon planets often employs an “all-or-nothing” approach, with a binary companion either “suppressing” planet formation altogether or allowing it to proceed completely undisturbed. However, works such as [Martin & Triaud \(2014\)](#) and [Martin & Lubow \(2017\)](#) have shown that if the disk survives, a binary companion may affect the

orientation and characteristics of that protoplanetary disk. Such an effect could manifest as different planet demographics around stars with binaries at intermediate separations: far enough to allow the disk to survive but close enough to modify the disk or resulting planets. Planet suppression changes steeply in the 1-50 AU separation range, so that it stands to reason that the planetary systems that *do* reside in these types of binaries illuminate the conditions under which planets can survive.

At present, incompleteness in our understanding of the rate at which binary systems host planets, as a function of their separation, hinders detailed study of planets detected by large transit surveys. ESA’s Gaia mission, with both astrometric and radial velocity observations, presents a novel opportunity to study binarity on a large scale. For example, [El-Badry et al. \(2021\)](#) identified 1.3 million spatially-resolved binaries from the Gaia catalog at the $>90\%$ confidence level. This type of analysis is timely for exoplanet science, as the increasing number of planets places increasing pressure on traditional time- and resource-intensive campaigns with adaptive optics ([Ziegler et al. 2018](#); [Ziegler et al. 2021](#)) or radial velocity follow-up ([Teske et al. 2021](#); [Chontos et al. 2022](#)). Out of necessity, observations to identify binary companions often focus upon known planet host stars, to eliminate false-positives or identify the effects of stellar contamination on inferred planet radius ([Ciardi et al. 2015](#)). The Sisyphean task of observing even a fraction of the stars in a transit survey like *Kepler* often means that campaigns must winnow this planet host star sample down yet further. To maximize scientific return, there is a strong incentive to focus resources upon the most scientifically interesting systems, such as those with multiple planets. For the study of exoplanets, Gaia presents a twofold opportunity to extract binarity information: first, it observes planet host stars in uniform way. Searches for stellar companions by ground-based means are shaped individually by survey completeness, which is itself informed by spectral resolution, stellar magnitude, and observing cadence. This naturally renders some portions of companion parameter space (mass ratio and orbital separation) much better studied for some stars than others, for which comparatively little is known. Secondly, Gaia observes *non*-planet-hosts in the same manner (a sample at least an order of magnitude larger still for transit surveys), enabling a precious field star comparison. Such comparisons are ultimately crucial for discerning the effects of stellar multiplicity upon planet occurrence at a demographic level.

To this end, we describe in this manuscript a technique to leverage available Gaia radial velocity data to investigate stellar binarity. As a complement to survey work with ground-based imaging and radial-velocity surveys, we have devised a probabilistic model to extract binary likelihood for every star with radial velocity observations from Gaia. Presently, only two quantities from these radial velocity observations are publicly available. These are (1) the number of observations and (2) the radial velocity “error”. The latter value is derived under the assumption of a constant radial

velocity model for the star, and thus will (we argue in this manuscript) increase when that assumption fails: namely, when the stellar velocity is not constant, but rather varying due to a companion. As yet, Gaia has not released the individual radial velocity time series measurements for most targets, and our understanding of binarity will ultimately be refined with future public data releases. Yet, we demonstrate here that binarity information is encoded in these two (at present) publicly available quantities, at a sufficient level for probabilistic measurements of binarity. On an individual stellar level, a probability extracted from two reported RV quantities has perhaps limited utility, but the same probabilities for every member of a large-scale survey of exoplanet host stars can be illuminating. While Gaia has gathered radial velocities for more than 7 million stars, in this paper we focus specifically upon the subsample of these stars observed by NASA’s *Kepler* and *TESS* missions. A total of 29,698 stars in the *Kepler* Input Catalog (about 15% of the total stars observed) possess Gaia radial velocity data, along with 854,652 stars in the *TESS* Input Catalog (about 9% of the total). This method is complimentary to astrometric binary detection methods using RUWE (Wood et al. 2021; Penoyre et al. 2022a,b; Andrew et al. 2022). Radial velocity methods are, by nature, more sensitive to close companions and equal mass binary systems. This manuscript is organized in the following manner. In Section 2 we describe our machinery for extracting the likelihood of stellar binarity from the publicly available radial velocity Gaia data. We assess our sensitivity to stellar companions as a function of mass ratio and orbital separation with a series of injection-and-recovery tests. In Section 3 we apply this machinery to the sample of *Kepler* and *TESS* Input Catalog stars with Gaia radial velocity data. We go on to validate our findings against important benchmarks. More specifically, we investigate how our sample of “likely binaries” overlaps with samples of binaries identified by other means. These means include the presentation of eclipses in photometry, the location on the HR diagram, and excess radial velocity noise from ground-based radial velocity surveys. In Section 3 we describe findings from the population of computed binarity probabilities in our sample. We touch upon a number of future scientific applications for these probabilities, including:

- Vetting of planet candidates and identification of false positives
- Comparison between distributions of planet- and non-planet-hosting stars
- Identification of circumbinary planet candidates
- Direct detection of sub-stellar-mass companions in the brown dwarf and giant planet mass range, and
- Examination of confirmed planetary systems with anomalous radial velocities.

This list is not complete, and we are hopeful that the catalog will be broadly useful to the community. While a detailed consideration of the effects of stellar multiplicity

upon planet occurrence is out of the scope of this paper, we hope that our findings will be applicable to that end. We summarize and conclude in [Section 5](#).

2. METHODS

The connection between radial velocity uncertainty and stellar multiplicity is well-known ([Maxted & Jeffries 2005](#); [Clark et al. 2011](#); [Maoz et al. 2012](#)). As RV surveys have evolved to observe hundreds of thousands to millions of stars within the last two decades, the method of using noisy, sparse radial velocity data to statistically characterize stellar multiplicity has evolved alongside them ([Price-Whelan et al. 2017, 2020](#)). The basic method begins with a simple assertion: stars have some intrinsic distribution of radial velocity noise that is created by internal processes. If this is true, single stars should form a Gaussian distribution of RV noise centered on a typical value. In the case where the source is an unresolved binary, semi-amplitudes for binary stars are generally in the 1-100 km/s range. Most internal processes do not create an RV signal on that scale. If the criteria for identification as a binary is set conservatively at 3σ , few single stars should be. The details of this operation are expanded upon in [Appendix A](#); in short, we have reduced the question of stellar binarity to this: does a source have RV noise in excess of the amount expected for similar-looking single stars?

The publicly available (as of EDR3) measurements for targets of the Gaia radial velocity survey comprise three values: (1) the median radial velocity, (2) the uncertainty on this median radial velocity, and (3) the number of Gaia radial velocity observations (called “transits”) used to quantify (1) and (2). The first two values are derived under the assumption that the measured radial velocities are attributable to a single star. Our procedure for extracting information about stellar binarity hinges upon a key assumption: that a radial velocity model for a single star will furnish a poor fit to a bona fide *binary* radial velocity curve. In the simplest case, this problem is akin to characterizing a sine wave with a single “median” value. The estimated uncertainty on the median value will correspondingly be inflated, since in this case the variability due to the underlying sine wave is (mis)characterized as “noise.” The degree to which a single star model will furnish a particularly “poor” fit, rendering the binary identifiable, is dependent upon several factors. These include the time sampling of the radial velocity curve and the properties of the binary itself, including mass ratio, orbital separation, eccentricity, and alignment relative to the line of sight. In this section, we describe our methodology for identifying likely binaries via the reported radial velocity uncertainty. In [Section 2.1](#) we detail our procedure for identifying anomalously high radial velocity errors, which is based upon a comparison among similar stars. In [Section 2.2](#) we characterize our sensitivity to binaries as a function of mass ratio, orbital separation, and stellar magnitude.

2.1. Binary detection & characterization

[Appendix A](#) and Foreman-Mackey, Chance, et al. (in prep.) describe our method of binary detection and characterization in more detail, but we also summarize the key results here. As discussed above, the *Gaia* catalog includes an estimate of the “RV error” for each RV target. Since this error is estimated by computing the sample variance of the RV time series, this value encodes information about both the per-transit RV measurement uncertainty and the excess RV variability introduced by companions.

To identify probable binaries in this sample, we first build a data-driven model to estimate the per-transit RV measurement uncertainty as a function of color and apparent magnitude (see [Appendix A](#) for more details), and then use this estimate to identify targets with statistically significant excess RV error. The key quantity that we compute is a p -value for each RV target in the sample under the null hypothesis of a single star time series. Informally, for a given target, this p -value quantifies the probability that such an extreme RV error would have been measured if the system were in fact a single star system with measurement uncertainty. Somewhat more formally, for a target n , this p -value can be written as

$$p_n = \Pr(\sigma > \sigma_n \mid \text{target } n \text{ is single}) \quad (1)$$

where σ_n is the observed RV error for target n . It’s important to note that this is not the same as quantifying the probability that a given target is a binary but, as we show below, it is a useful quantity for selecting candidates. In the following sections, we identify probable candidates by selecting targets with p -values below 0.001, and then calibrate the sensitivity of this method using injection and recovery tests.

Beyond identifying likely binary candidates, we also place probabilistic constraints on the RV semi-amplitude for each target, under the assumption that the RV variations can be described by Keplerian motion. The details for this procedure are described in [Appendix A](#), and in [Section 3.3](#) we demonstrate the accuracy and precision of these measurements when compared to spectroscopic binaries detected by targeted RV surveys.

2.2. Injection and Recovery Analysis

We summarize here an injection-and-recovery analysis to investigate our sensitivity to stellar binarity, within the framework we outline in the previous section. To this end, we create a synthetic population of binaries, which we “observe” at a typical Gaia cadence and with typical Gaia per-measurement radial velocity uncertainty. We then calculate the median radial velocity and radial velocity error of these “observations”, to obtain a synthetic data set that resembles the reported radial velocity Gaia data. Given a ground truth knowledge of the population, we can then assess the ability of our machinery to correctly identify sources of anomalously high radial velocity error. In [Section 2.2.1](#), we describe the impact of Gaia sample selection on this empirical sensitivity map.

First, we draw our underlying stellar binary properties with uniform log spacing in semi-major axis, a , and in mass ratio, q . Our range in q spans 10^{-4} to 1, which for a Sun-like star brackets a range with a Jupiter-mass exoplanet at one extreme and an equal mass stellar companion at the other. Our semi-major axis range spans 10^{-2} - 10^3 AU, but our sensitivity falls off substantially for $a > 1$ AU. Within this $\{q, a\}$ parameter space, we generate one million binary star pairs. We then assign orbital inclination relative to the line of sight, orbital eccentricity, and longitude of periape from uniform distributions of $\cos 0 - \cos \pi/2$, 0-1, and 0 to 360 degrees, respectively. Next, we calculate the binary’s orbital period and employ Kepler’s equations to solve for the positions and velocities of the two stars. The number of synthetic observations n is drawn from the distribution of RV transits shown in Figure 1. This depicts the distribution in the number of transits for the observed Gaia stars in the *Kepler* Input Catalog and the *TESS* Candidate Target List. We “measure” the radial component of the velocity at uniform random times t_n over the 668 day observing time span of EDR3. We also calculate the semi-amplitude of the heavier (and presumably brighter) component.

We add realistic per-measurement radial velocity error as follows. First, we partition the real observed *Gaia* catalog stars into bins in color-magnitude space. For each of these bins, we tabulate the average radial velocity error. We randomly assigning each simulated stellar pair to a color-magnitude bin, and draw our per-measurement error from the observed underlying distribution for that bin. This procedure has an important caveat. In the idealized case, the radial velocity noise distribution in each color-magnitude bin would correspond to a population of single stars, with individual error budget dominated by the measurement noise from *Gaia*’s spectrograph. However, in practice each bin also contains *bona fide* binaries. In these cases, the observed Gaia RVs may in fact be dominated by the reflex motion of the stars, and associated “noise” may in fact be inflated. In this sense, our sample of “control” stars is contaminated by some binaries. Other stars will have intrinsically higher amounts of RV noise for reasons unrelated to a binary companions. We seek to mitigate this contamination by using a very conservative definition to detect “outliers”: at the $>3\sigma$ level from the mean in each bin. While this decision leaves us with a significant false-negative rate, it also means that we can be reasonably certain that our detections represent significant levels of noise.

We then run **paired** (as described in Appendix A) on this simulated sample of binary stars, with our results depicted in Figure 2 as a function of semi-major axis and mass ratio. The recovery rates with overplotted 99% recovery rate contours are depicted by white contours corresponding to 5 different *Gaia* magnitudes. We are most sensitive to binaries near equal mass, recovering $> 80\%$ for all magnitude bins. We find that our recovery rate drops steadily with mass ratio, but more quickly with separation.

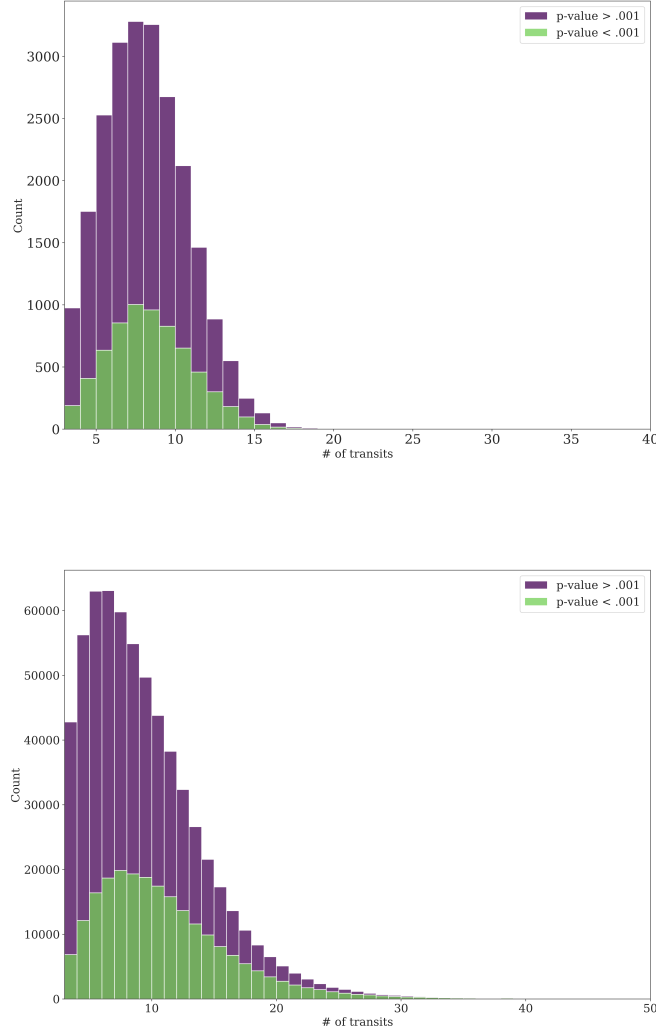


Figure 1. *Top:* A histogram of the number of RV observations (transits) of sources in the KIC crossmatch. *Bottom:* Identical plot for the TESS Community Target List. The CTL sources tend to have more observations on average, along with a longer tail toward more observations.

The results of this injection-and-recovery test indicate that we have some sensitivity to brown dwarfs around bright stars ($m_g < 7$) out to a few AU ($\log q$ of -1.1 for a Sun-like star). Around those same stars, we are sensitive at the 99% confidence level to mass ratios of $q=0.1$ at 10 AU. It is outside the scope of this work to compare raw binary occurrence to other works, but we note (per [Duquennoy & Mayor 1991](#)) that 10 AU for a G dwarf corresponds to an orbital period of $P \sim 10^4$ days, where 90% of companions to G dwarfs have $q > 0.1$. We therefore possess modest completeness to stellar companions to bright G dwarfs. Specifically with respect to known planet hosts, while the recovery rate drops off steeply with magnitude, we retain the ability to detect stellar mass companions ($q > 0.1$) interior to 1 AU around Sun-like stars

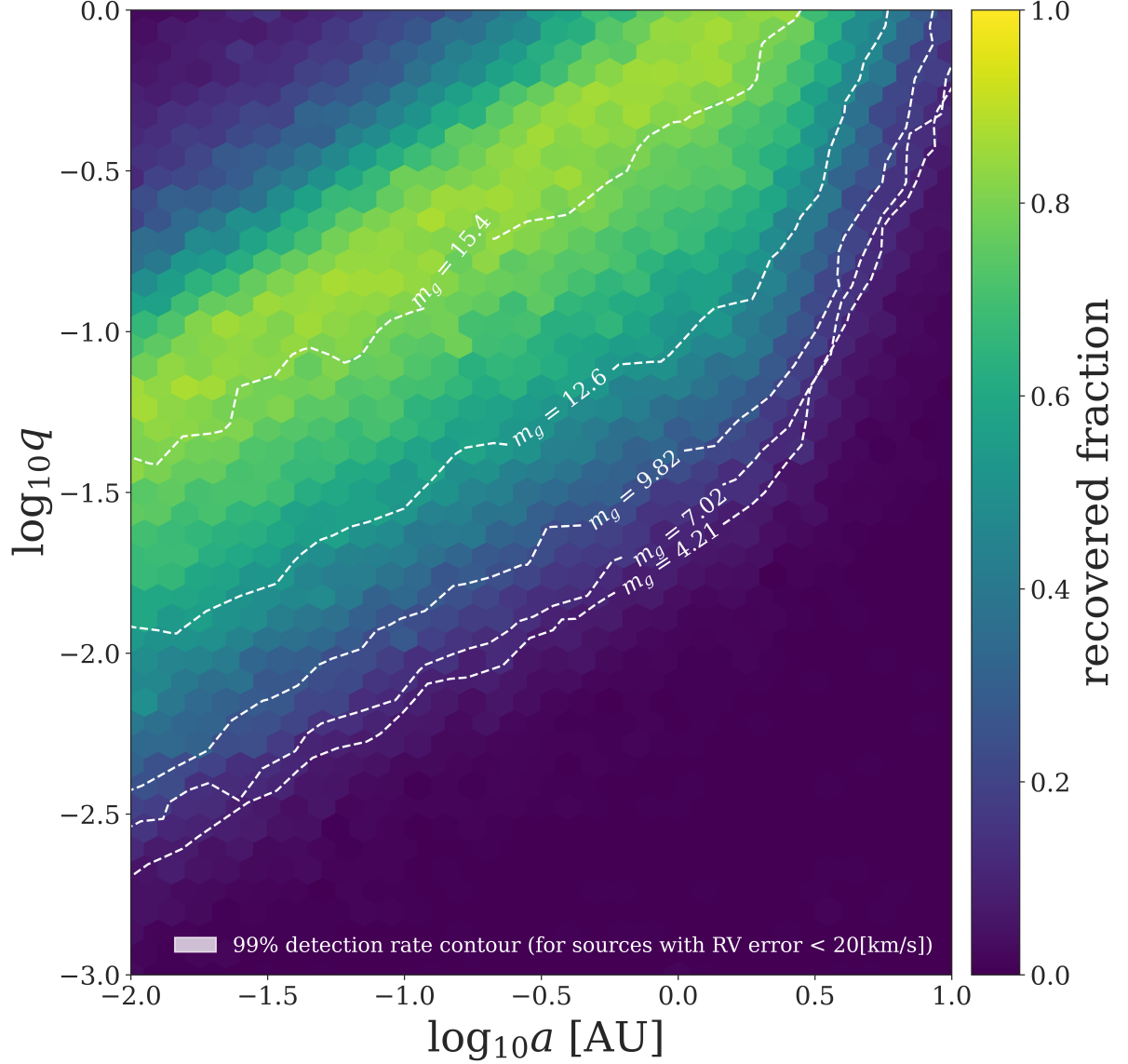


Figure 2. Detection efficiency using RV errors as a function of injected separation and mass ratio. The 99% recovery rate is shown for different mean apparent magnitude contours. The color of each hexbin indicates the median p-value for pairs in that bin.

down to m_g of 12.6 with 99% confidence. While Gaia only gathers radial velocity observations for a fraction of its targets, we comment briefly on our empirical sensitivity as it applies to the population of transit candidate host stars. This fiducial magnitude cutoff of $m_g \geq 12.6$, where we reliably recover stellar companions to Sun-like stars interior to an AU, corresponds about half of the host stars to Kepler Objects of Interest (Coughlin et al. 2016, hereafter KOIs). Roughly 80% of the TESS Observations of Interest (TOIs) from the primary mission and 20% of TOIs from the Faint Star catalog (Guerrero 2021; Kunimoto et al. 2022) are brighter than this magnitude threshold (here we have converted *TESS* and Gaia magnitudes per Stassun et al. 2019). We conclude from our injection-and-recovery analysis that, for the fraction of

transit host stars with radial velocity observations from Gaia (described further in [Section 3](#)), **paired** is capable of detecting close stellar companions and occasionally substellar companions.

2.2.1. *Completeness to equal-mass, short-period binaries*

There is an additional consideration for our injection-and-recovery analysis, related to sensitivity in the portion of $\{a, q\}$ space corresponding to short period binaries with mass ratios q near to 1. While we would *a priori* expect our sensitivity to peak in this corner of binary parameter space, we note that sources with radial velocity errors >20 km/s are culled from the Gaia sample of radial velocity stars and not reported. This down-selection necessitates a careful consideration of the **paired** sensitivity map when comparing to known samples of binaries, in the following way. Given a hypothetical sample of 1000 *Kepler* stars of equivalent brightness and an underlying rate of binarity of 50%, we might expect 10% of this sample to be Gaia radial velocity targets. These would be selected randomly, so that we could employ **paired** to interpret the Gaia RV data of 100 stars out of the original 1000. In the simplified case of uniform sensitivity to all binaries, we might expect **paired** to report that approximately 50 stars of the 100 are “likely” binaries, reflecting the true underlying rate. However, in the case of down-selection of the stars with highest apparent RV noise, perhaps the 10 most obvious binaries of the 50 are culled from the table of the stars with radial velocity data from Gaia. Among the 90 in the subsequent public sample, **paired** would detect the remaining 40 binaries, but the interpretation of a 40/90 (45%) underlying binarity rate would be incorrect. We anticipate that a comparison of **paired** against known binary catalogs will always *underestimate* the true rate for this reason. The degree of that underestimation depends upon the fraction of binaries “obvious” enough to be culled from the catalog.

3. RESULTS

In the previous section, we assess our theoretical sensitivity to binaries with the machinery of **paired**. In this section, we describe our findings from running **paired** on the 9% of the *Kepler* Input Catalog (29,698 stars) and 15% of the *TESS* Input Catalog (854,652 stars) with EDR3 radial velocity observations. Below, we compare our sample of “likely” binaries from this exercise against existing benchmark indicators of binarity, to assess the extent to which the outliers in radial velocity noise we are detecting are *bona fide* stars in binary systems. We first consider **paired**’s performance on the highest fidelity sample of individually identified eclipsing and spectroscopic binaries ([Section 3.1](#)). We then turn to the results of large stellar surveys, where indicators of binarity include position on the HR diagram ([Section 3.2](#)) and radial velocity semi-amplitude ([Section 3.3](#)).

3.1. *Validation Against Catalogs of Known Binaries*

We construct a “likely binary” catalog by selecting all cross-matched KIC and CTL targets with a p -value (described in [Section 2](#)) below 0.001 (6,630 and 329,712 sources, respectively). We emphasize that the p -value is *not* the same quantity as the false positive rate of binarity, but rather the likelihood that the source’s radial velocity noise is indeed anomalously high compared to stars of similar color and magnitude. A calibration of the latter quantity with the rate of “false positives” would depend on the true fraction of both binaries and astrophysical sources of false positives, which is beyond the scope of this work. [Figure 3](#) shows the cumulative p -value distributions for all of our cross-matched sources. We find that approximately 22% of the KIC and 38% of CTL stars exhibit excessive radial velocity noise at the $p < 0.001$ level.

Known eclipsing binaries (EBs) in the *Kepler* and *TESS* catalogs present an ideal sample for testing *paired*’s performance. They comprise the types of edge-on and short period systems to which we claim high sensitivity (per [Section 2.2](#)), and can be confirmed as binaries independent of spectroscopic measurements. We expect our rate of recovery to be similar when comparing to the *Kepler* and *TESS* eclipsing binary catalogs. This is because, While *TESS* stars are brighter on average than *Kepler* stars, eclipsing binaries reside in the part of $\{a, q\}$ space where we retain high recovery rates even for dim ($m_g > 15$) stars. Our recovery rate will depend on a combination of factors: the distribution in $\{a, q\}$ space of the detected eclipsing binaries (itself a function of the underlying transit survey sensitivity), our detection efficiency over that range, and the magnitude distribution of the stars.

Indeed, we find that for the 331 EBs in the *Kepler* EB catalog crossmatch (containing 2922 sources) that we have at least 3 RV transits for ([Kirk et al. 2016](#)), 73.8% exceed the $p < 0.001$ threshold. For the 458 EBs in the *TESS* EB catalog crossmatch (containing 4584 sources) ([Prša et al. 2022](#)) we recover 73.1% as binaries.

Our recovery fraction is modestly higher for spectroscopic binaries. As a point of comparison, we perform a cross-match with the SB9 catalog ([Pourbaix et al. 2009](#)). Of the 1669 single-lined spectroscopic binaries with more than 3 RV transits included in ([Pourbaix et al. 2009](#)), we recover 82.8%. We estimate that this higher recovery rate is attributable to the similarities between our sensitivity curve (reliant upon radial velocities) and a radial velocity survey, as compared to the relationship between our sensitivity curve and that of a transit survey.

3.2. Location on the Hertzsprung Russell Diagram

[Figure 4](#) shows the median p -value of targets in bins on the color-magnitude diagram for our KIC and CTL crossmatches. The yellow bins indicate an area that (as a rough estimation) has a high fraction of binaries. From this diagram, it can be seen that the expected features of an equal-mass binary main sequence and increasing binary fraction with mass are present in both catalogs.

3.3. Comparison to radial velocity catalogs

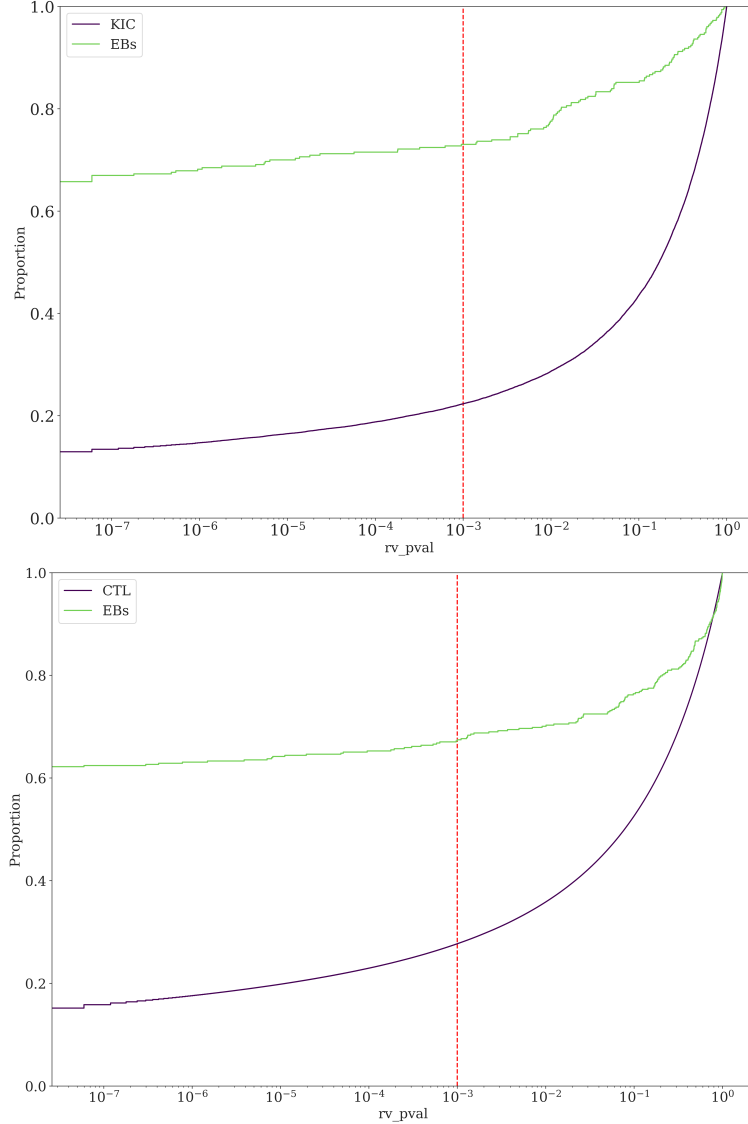


Figure 3. Left: CDF of p-values of KIC crossmatch and Villanova Kepler Eclipsing binary catalog (Kirk et al. 2016). The red dashed line is our $p < 0.001$ threshold. The intersection of this line with the CDFs is the proportion of the sample that are flagged as binaries. Right: Identical plot for the TESS Community Target List and Villanova TESS Eclipsing binary catalog (Prša et al. 2022). Eclipsing binaries from both catalogs have excess RV noise that meets our threshold in $\sim 70\%$ of stars compared to the “field” rate of $\sim 20\%$.

For roughly 35% of sources, we calculate the probability distribution for the radial velocity semi-amplitude as described in Appendix A. Inferred semi-amplitude posteriors from sparsely sampled data generally have long tails, accommodating the possibility of larger eccentricity values (Price-Whelan et al. 2017).

Predictably, agreement between our method and other RV surveys increases with semi-amplitude. The vast majority of the crossmatched RVs are in agreement to $1\text{-}\sigma$ (see Figure 5)(Price-Whelan et al. (2020), Price-Whelan, in prep.). Our ability to infer a semi-amplitude degrades near the *Gaia* RV noise floor of about 1 km/s. Lower than that, the RV signal is indistinguishable from noise. We also lose sensitivity at

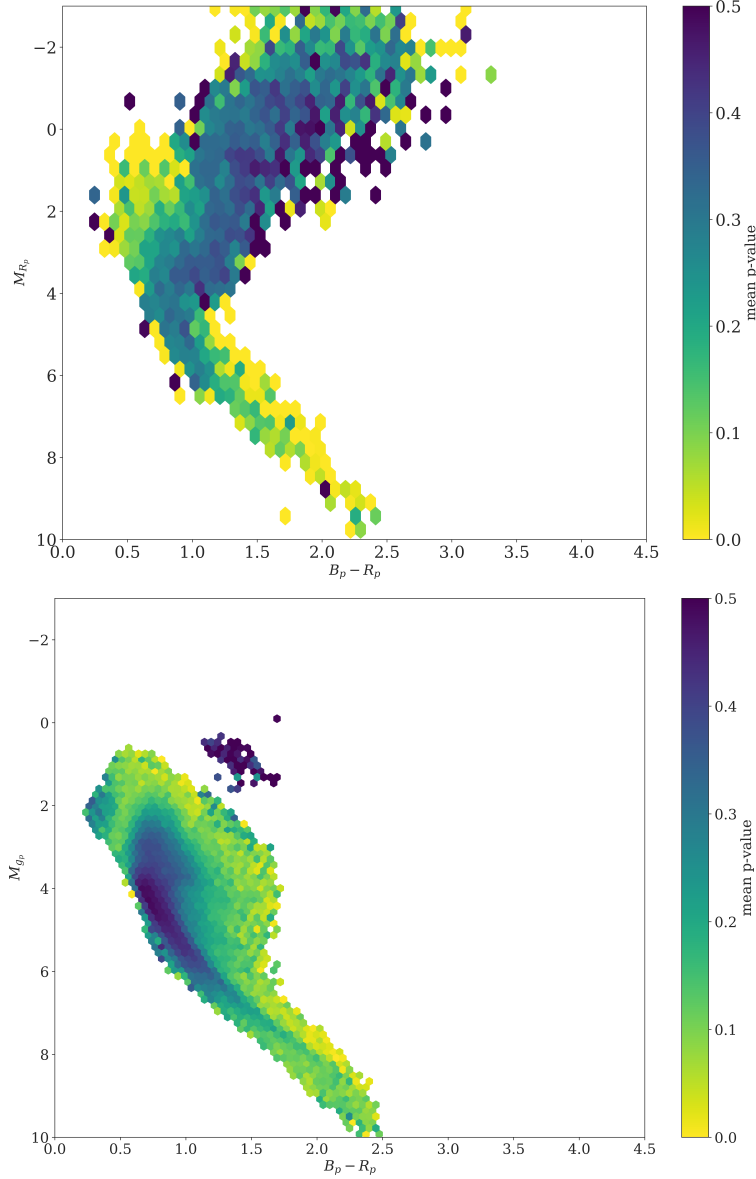


Figure 4. *Top:* A color-magnitude diagram of our cross match with the KIC covering 29698 stars. *Bottom:* A color-magnitude diagram of our cross match with the CTL covering 854652 stars. The color corresponds to the median p -value for that hexbin, with yellow (zero) indicating a high fraction of binaries. We can see both the binary main sequence and the increasing binarity with decreasing color.

higher semi-amplitudes because these objects are generally removed from the Gaia catalog because of the large RV error.

4. ANALYSIS

4.1. Exoplanet Candidate Vetting and Identification of False Positives

One of the anticipated uses of our catalog is in vetting exoplanet candidates. Currently, one of the procedures for transforming a transiting planet “candidate” to a confirmed planet is a follow-up RV campaign. Where possible, a measured planetary

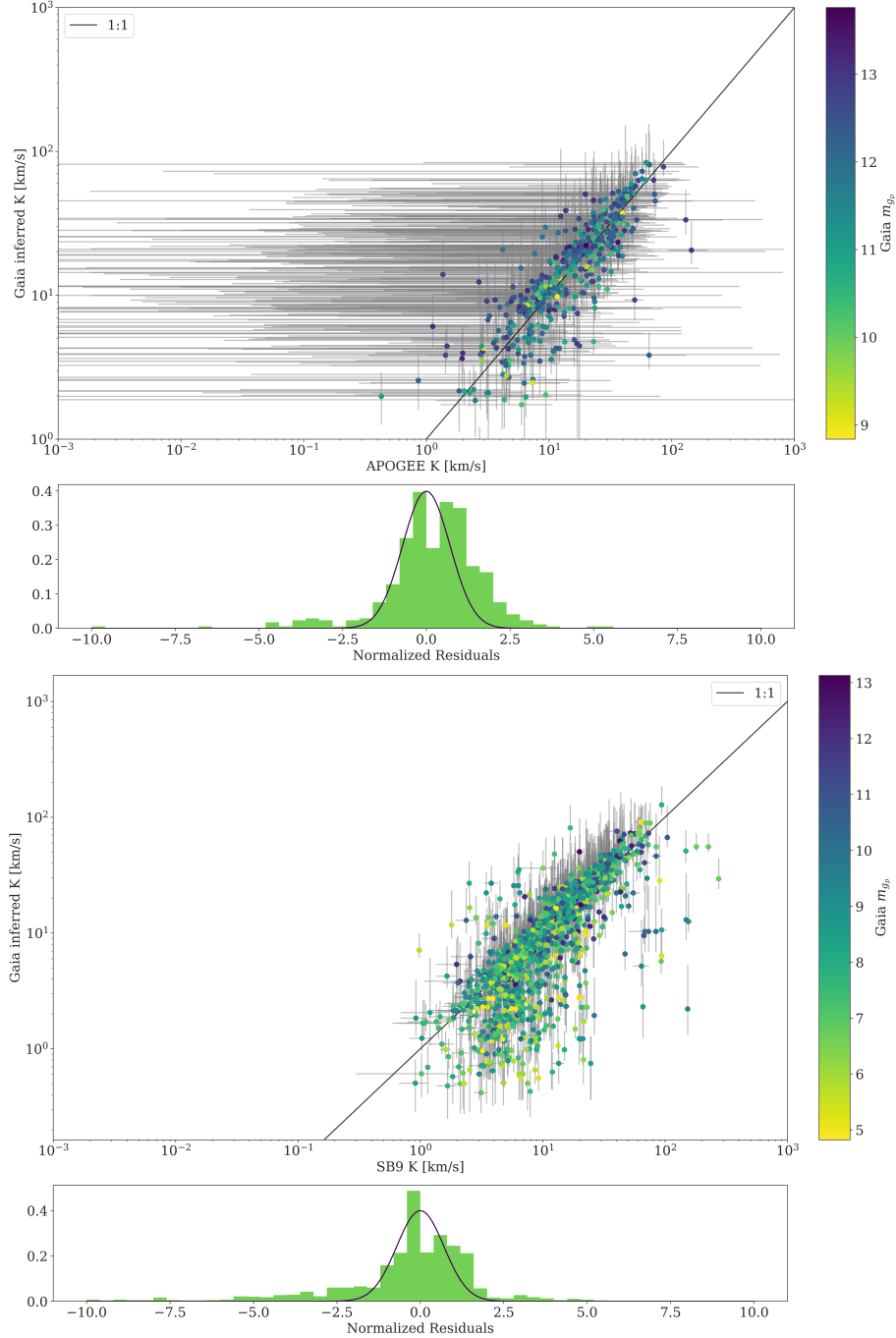


Figure 5. Here we compare with the ground based mid-resolution RV surveys APOGEE (top) and SB9 (bottom) for all the sources where we have overlap with our catalog and can constrain semi-amplitudes. There is tight agreement for high semi-amplitudes that stars to loosen as K approaches Gaia’s noise floor of ~ 1 km/s.

mass is ideal, but such campaigns can also simply confirm (by a *lack* of sizeable RV variations) that the transit signal is not being caused by a grazing eclipsing binary.

The ability to pre-sort planet candidates by p-value into likely false positives and *bona fide* candidates would enable follow-up resources to prioritize the most promising candidates without taking a single RV measurement. There also exists a retroactive

application. Candidates which were statistically validated may warrant a revisit if they have low p-values that indicates a high-mass companion.

4.2. *Potential sources of false positives*

We emphasize here that a p-value calculation cannot be interpreted as the false positive rate for our sample; these quantities are distinct and should not be conflated. A known source of false positives is rapidly-rotating stars. The rotational-broadened spectral lines of stars with $v \sin i > 10$ km/s can lead to an over-estimation of the RV measurement error from a source. There is no way to distinguish this from RV noise from a companion, therefore rapid rotators are likely to be flagged as binaries. A careful reexamination of the assumption that σ_n is constant at a given color and magnitude may disentangle this noise from that more likely to be caused by companions, but that is outside of the scope of this paper.

4.2.1. *Differences between the Kepler and TESS catalog*

The cross match with Kepler contains 29,698 matches out of nearly 200,000 Kepler target stars, down to a Gaia g magnitude of 14.84. The relatively low fraction is a result of removing stars without a minimum of 3 RV transits. The cross match with *TESS* contains 854,652 out of approximately 9.5 million stars in the Candidate Target List, down to a Gaia g magnitude of 15.81. The sources in the KIC crossmatch on average have fewer RV transits than those in the CTL list. Recall that Equation A1, ϵ_n is proportional to this number. In essence, while the median number of transits is similar, some of the CTL sources are far more well sampled than the KIC sources. The *Kepler* Object of Interest catalog has been repeatedly and thoroughly (statistically, in most cases) vetted for false positives. The *TESS* Object of Interest catalog is still being added to with follow-up observations and vetting on going. Combined with a more lax policy for disposition as a planet candidate (Guerrero 2021), the TOI planet candidates are much more likely to be an astrophysical false positive. The side-by-side comparison of the two catalogs in Figure 6 is revealing in this aspect. There is a clear difference between the p-values of planet host and non-hosts for *Kepler*, but the populations look quite similar for *TESS*.

4.3. *Binary probabilities of planet host stars and field stars*

Calculating occurrence rates is a non-trivial problem, especially when using a collection of surveys all with varying sensitivity constraints. What we will present in this paper serves as more of a crude guide to what we should expect to see in a full treatment. Although our results are only a statistic and not the actual binary fraction of stars, it should be close enough for quiet main-sequence stars. Previous studies of close binaries hosting exoplanets (Wang et al. 2014; Moe & Kratter 2021) have established that the presence of a close binary is deleterious to planet formation. Particularly in the case of systems that have stellar companions within 10 AU, the fraction of planet hosts decreases precipitously. With that information in hand,

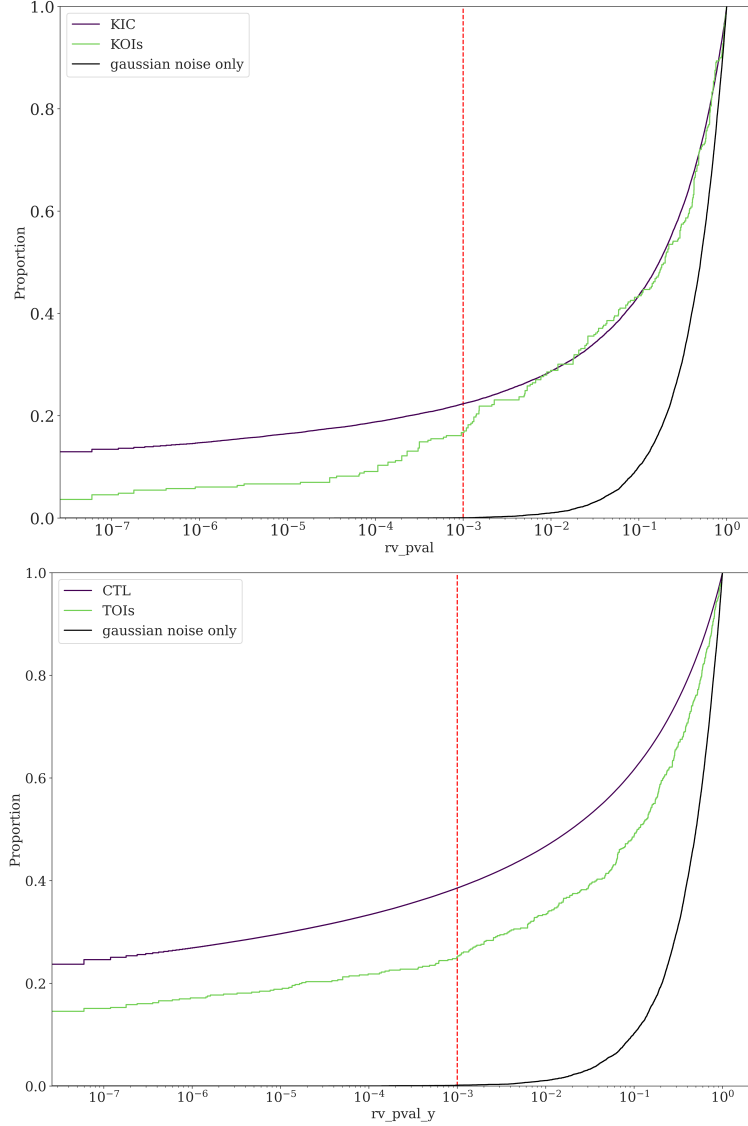


Figure 6. *Top:* CDF of p-values of the KIC crossmatch and KOI catalog (exclusive of known false positives). The red dashed line is the threshold for determining a star is a binary. The intersection of this line with the CDFs is the proportion of the sample that are flagged as binaries. The most striking feature of this plot is the reduction in the proportion of low p-value systems hosting planets can be seen starting near the cutoff value of 0.001. *Bottom:* Identical plot for the TESS Community Target List and TOI catalog (Guerrero 2021). The TOI catalog (with known false positives removed) appears to be substantially more contaminated with false positives than the KOI catalog.

we expect to see that reproduced using our method of establishing stellar binarity. In the left panel of Figure 6 we present the cumulative distribution functions of our crossmatch with the Kepler Input Catalog (KIC) and the Kepler Objects of Interest (KOIs). We have removed candidate planets and known false positives in order to use the KOIs as our sample of planet hosts. Figure 6 shows the distribution of the selected stars binary p-values where values closer to 0 indicate increasing likelihood of being a binary. These plots can also be read as a kind of percentile ranking of the

excess RV noise from each target. Our relatively conservative limit of 10^{-3} or 99.9th percentile of RV noise for binary classification should exclude the vast majority of targets that have excess RV noise by chance. We note 2 important features. First, while the two CDFs are quite similar approaching the cutoff as they descend in p-value, after the cutoff their behavior diverges. The number of KOI targets classified as binaries sharply decreases relative to the KIC targets. This decrease is also insensitive to our choice of classification limit. We interpret this feature as the expected decrease in the number of planet hosting systems in close binaries. Second, there is a slope as the p-values approach zero. Smaller p-values (and therefore larger signals) generally indicate higher mass ratios and smaller separations. We therefore interpret this feature as systems hosting larger and/or closer companions are less likely to host a KOI. These findings are consistent with the observation that close binaries suppress planet formation. This suppression is not, however, complete. Investigating systems that appear to host a massive companion while also hosting planets has the potential to more precisely determine what mechanism this suppression operates by examining the surviving systems.

4.4. *Direct detection of sub-stellar-mass companions*

Our machinery, when applied to the Gaia data, has marginal sensitivity to both gas giants and brown dwarfs at short periods. These objects, while not meeting the $p < 0.001$ threshold we have set for stellar binaries do create signal at the $p \sim 0.01 - 0.1$ level. This group of host stars will be 10 to 100x more contaminated than our stellar binary even if our simple assumptions hold. Our interpretation of this peak for sub-stellar objects at $p = .1-0.1$ relies upon our assumption for how p-values scale with our recovery rate as shown in Figure 2. If recovery rate scales with p-value as shown, we can estimate, for example, that $\sim 50\%$ of $pval = 0.01$ signals are generated by companions.

To test this hypothesis, we used a population of known massive hot Jupiters. For a selection of hot Jupiters with the largest semi-amplitudes, there is a noticeable excess when compared to the rate for the entire sample Figure 7, as we would expect if we are detecting sub-stellar objects. We also see a steep decline in the fraction of lower p-values, which we would expect given that hot Jupiters are unlikely to have close stellar companions creating clear signals (Knutson et al. 2014; Piskorz et al. 2015; Ngo et al. 2015). The juxtaposition of these two features implies that they are produced by sub-stellar companions. Even if we cannot confidently call this a detection individually from the Gaia RVs alone, we suspect that an RV search of these targets would prove fruitful.

4.5. *Identification of circumbinary planets*

This catalog has the potential to uncover examples of one of the more elusive planet formation outcome: misaligned circumbinary (or P-type) planets. Despite the thousands of known exoplanets and indications that they should be just as common as

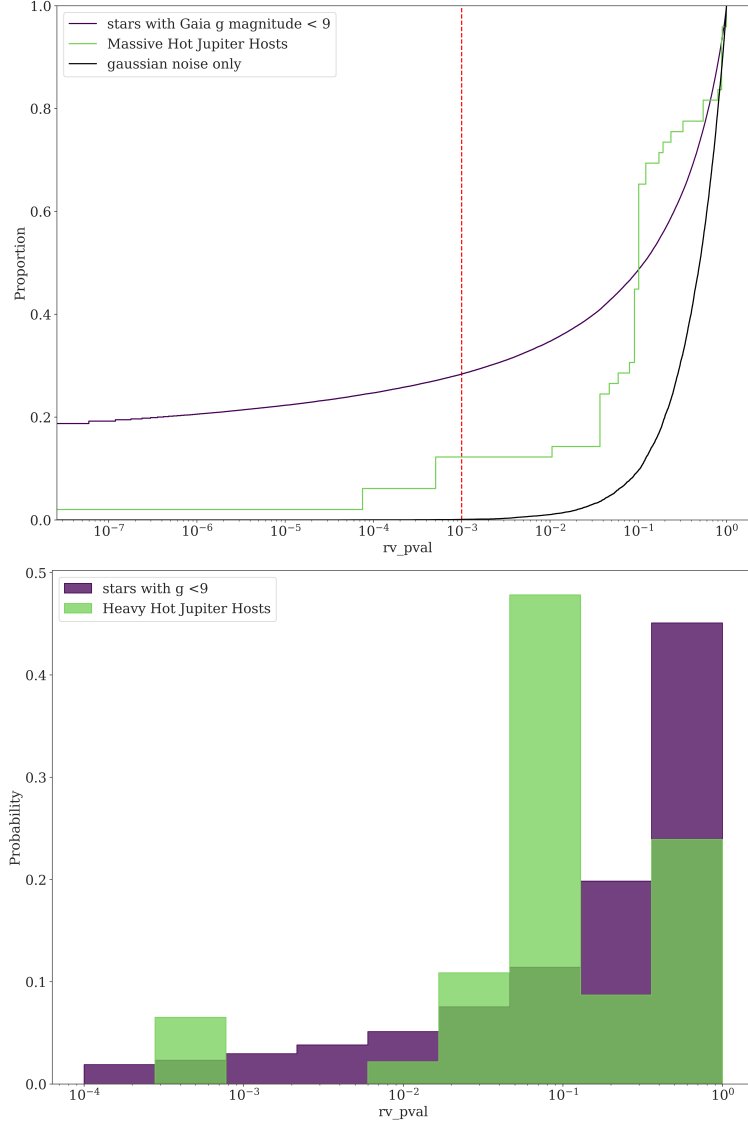


Figure 7. The distribution of p-values for bright massive hot Jupiter hosts. Despite the low number of host stars in the sample (21), there is a clear excess of 90th percentile-level RV noise, possibly from their previously known planets.

planets orbiting single stars (Martin & Triaud 2014), only 12 transiting circumbinary planets are currently known (Kostov et al. 2020). The fact that we only know of a small number of systems therefore must be reflective of some combination of intrinsic and observational biases. For the most part, we only know that the host stars are in a close binary because they eclipse one another. Examinations of protoplanetary disks around young binary stars indicates that $\sim 70\%$ of these disks are aligned with the binary for periods of less than 20 days, but the range widens all the way to polar configurations for periods greater than 30 days (Czekala et al. 2019). Circumbinary systems where this is not the case have to date not been identified as such. For misaligned circumbinary systems, epochs where no transit occurs are the majority (Chen & Kipping 2021). The case of two or more transits per epoch is one

way to unambiguously identify a circumbinary planet, but this only occurs $\sim 3\%$ of the time. These systems may make up some portion of systems with single observed transits. Using this catalog is a viable way to identify systems in this configuration. Conditioning a search for these planets on evidence that a given planet host is a close binary drastically reduces the amount of target light curves that need to be searched.

Planets hosts that are flagged as binaries, especially those with inferred semi-amplitudes indicating a close binary, represent the best candidates for being a mis-aligned CBP. Worthy of particular scrutiny is KOIs meeting those criteria that have only one or two planet transits present in their light curves. The vast majority of CBPs that have the potential to transit do so only in a “sparse” configuration (Martin & Triaud 2014), where non-consecutive transits are the norm. Many searches of the kepler catalog for these single or sparsely transiting planet candidates have already been conducted (Wang et al. 2015; Foreman-Mackey et al. 2016; Uehara et al. 2016). The combination of this catalog and known single-transit planet candidates may prove key in finding one of this as-yet unseen type of planetary system.

Table 1. Kepler planet host candidates of particular interest with semi-amplitude ranges inferred from *Gaia* RVs. KOIs that meet the p-value threshold but have effective temperatures greater than 6250K are removed.

KIC	KOI	# of RV transits	K_{16th}	K_{50th}	K_{84th}	KOI Disp.	Gaia m	T_{eff}
3440118	K03876	9	11.828	15.255	25.527	CP	12.605	5620
4056616	K02013	7	6.665	9.03	16.42	CP	13.197	4507
5450893	K02970	9	13.244	17.522	28.727	CP	12.769	6046
6289257	K00307	8	7.181	10.87	19.08	CP	12.757	6023
8240797	K01809	6	11.258	15.67	29.812	CP	12.746	5772
8711794	K00105	6	5.835	9.846	19.335	CP	12.853	5666
9489524	K02029	11	6.118	8.562	13.435	CP	12.95	5208
3733628	K00387	13	9.098	11.534	18.12	CP	13.364	4538
7742408	K03478	8	11.557	15.131	26.124	CP	13.351	4928
5511081	K01930	12	4.042	5.837	8.89	CP	12.076	5951
6021275	K00284	6	5.157	8.466	16.42	CP	12.32	5931
7419318	K00313	7	19.866	25.682	46.373	CP	12.931	5188
7584650	K02631	5	26.003	37.206	77.673	CP	13.437	5871
9450647	K00110	11	5.111	8.457	13.517	CP	12.584	6215
7749773	K02848	7	4.169	7.087	12.983	CP	12.423	5691
8424002	K03497	6	6.083	8.994	17.637	CP	13.317	3419
9886361	K02732	12	6.152	9.117	14.103	CP	12.752	6170
10212441	K02342	6	13.355	19.138	36.643	CP	13.041	5798
11086270	K00124	12	4.873	8.545	13.538	CP	12.891	5869
11764462	K01531	7	11.699	16.585	28.956	CP	13.122	5646

Table 1 continued on next page

Table 1 (*continued*)

KIC	KOI	# of RV transits	K_{16th}	K_{50th}	K_{84th}	KOI Disp.	Gaia m	T_{eff}
11760231	K01841	10	7.892	11.024	18.273	CP	13.242	5187
9579641	K00115	7	6.793	10.981	20.165	CP	12.794	5779
9881662	K00327	7	13.075	18.197	31.932	CP	12.932	5945
10063208	K04292	11	8.925	11.879	19.089	CP	12.833	5525
10528068	K01162	6	6.11	10.292	20.193	CP	12.722	5751
11446443	K00001	5	3.999	5.982	12.741	CP	11.283	5820
11017901	K01800	10	4.361	6.428	10.578	CP	12.375	5494
11551692	K01781	7	2.681	4.153	7.424	CP	12.226	4920
12301181	K02059	7	23.879	30.858	58.983	CP	13.225	4997
12785320	K00298	5	12.129	18.065	37.831	CP	13.208	5250
1025986	K07621	6	3.363	4.57	9.213	PC	10.06	5604
1161345	K00984	5	3.169	5.761	12.179	PC	12.391	5296
3129238	K07645	11	3.51	5.273	8.401	PC	12.321	5341
3545478	K00366	6	3.626	6.516	12.631	PC	11.556	6201
6309307	K05262	9	2.981	4.175	6.824	PC	12.342	4973
4276716	K01619	6	3.457	4.92	9.726	PC	11.801	4830
5802205	K08107	8	1.808	3.095	5.392	PC	11.022	6180
7901016	K04257	6	6.65	12.748	24.783	PC	13.355	5745
8702537	K07905	7	6.238	10.191	18.693	PC	13.045	5616
10287723	K01174 ^a	10	9.423	12.102	20.392	PC	13.428	4500
10352333	K03991	8	12.876	17.388	29.455	PC	13.183	5519
10163067	K07291	8	11.201	14.659	25.408	PC	12.574	6167
4139254	K06108	10	35.969	44.797	67.957	PC	12.072	5571
4141593	K07685	7	21.097	27.676	50.725	PC	13.251	5999
4450844	K03168	7	3.167	4.268	7.642	PC	10.455	5843
5857656	K05205	5	13.355	19.689	41.405	PC	12.771	5861
5858919	K08109	11	2.086	2.688	4.307	PC	11.882	3297
8009811	K05459	7	2.631	4.275	7.669	PC	11.419	6039
7661893	K04296	8	31.578	39.644	67.002	PC	12.997	5615
8873090	K02968	13	3.407	4.677	7.071	PC	11.422	6133
9330740	K05656	17	6.516	8.645	12.801	PC	12.652	5717
9072639	K04198	6	16.049	21.63	41.245	PC	12.55	6017
8005002	K05457	8	3.298	5.352	9.242	PC	12.422	5146
9469494	K07938	11	13.172	16.385	26.321	PC	11.655	5989
10736489	K07368	9	8.596	11.287	19.17	PC	12.831	5227
11182260	K07415	9	35.532	44.791	69.626	PC	13.247	4995
11182706	K08046	12	3.158	4.58	7.123	PC	12.619	4859
11600299	K05916	7	2.184	2.984	5.342	PC	12.052	3661
11502218	K00970	17	35.866	41.432	56.48	PC	6.948	4813

Table 1 *continued on next page*

Table 1 (continued)

KIC	KOI	# of RV transits	K_{16th}	K_{50th}	K_{84th}	KOI Disp.	Gaia m	T_{eff}
12170767	K05960	8	23.423	29.814	52.671	PC	13.3	5539

^aSingle transit

4.6. Confirmed planetary systems with anomalous radial velocities

Here we highlight a few systems that may warrant a closer look in light of their known system characteristics and high binary probabilities.

4.6.1. Kepler-411

Kepler 411 has an inferred RV semi-amplitude of $4.15^{+3.27}_{-1.47}$ km/s and a p-value of 2×10^{-4} placing it in the 100th percentile of excess RV noise of similar looking stars. The system was characterized in Sun et al. (2019). the outermost known transiting planet, Kepler-411d is seen to have a strong interaction with with an outer, non-transiting perturber. This investigation constrained the mass of planet e to $10.8 \pm 1.1 \oplus$, assuming that the system was co-planar. However, TTV inversion for exterior, non-transiting perturbers is a fraught exercise. The system also sits well above the single-star main sequence in a color-magnitude diagram. Given the limited quality of the TTV data, it is difficult to eliminate the possibility of a more massive inclined companions being responsible for planet d’s TTVs.

4.6.2. Kepler-132

Kepler-132A has an inferred semi-amplitude of $8.46^{+7.96}_{-3.31}$ km/s and a p-value of 3×10^{-4} placing it in the 99.9996th percentile of excess RV noise of similar looking stars. The system was briefly mentioned in Lissauer et al. (2014) because of a curious characteristic: It is a double star of two nearly equal magnitude F7 components and two of the planets cannot possibly exist while orbiting the same star. KOI-284.02 and 284.03 have periods of 6.41 and 6.17 days, respectively. While EDR3 only has an RV measurement for the slightly brighter component, recon spectra has indicated that the stars had an instantaneous difference in radial velocity of about 1 km/s (Lissauer et al. 2014). The two stars have a projected separation of 450 AU. It is unlikely that the motion of these two stars over the EDR3 observing baseline is causing the excess RV noise.

4.6.3. Kepler-410A

Kepler-410A has an inferred RV semi-amplitude of $1.72^{+2.57}_{-0.87}$ km/s. This system is unusually bright (Gaia G magnitude of 9.38) so we can expect the Gaia per-transit RV uncertainty to be around 100-200 m/s. This signal cannot be explained by the known companion Kepler-410B, an M dwarf with a period ~ 2500 years. This system has previously been investigated and thought to possibly be host to another stellar

component (Gajdoš et al. 2017). Follow-up RV observation have ruled out a stellar mass companion.

4.6.4. KOI 1174

KOI 1174 has an inferred RV semi-amplitude of $12.10^{+8.29}_{-2.68}$ km/s and a p-value less than 10^{-6} . The system has a single observed transit with a depth indicating a radius of $2.99R_{\oplus}$. Single-transit objects are of particular interest because they possibly represent detection of circumbinary planets misaligned with their host stars. Such planets are not expected to transit periodically, making them difficult to identify. Despite this, non-eclipsing binaries make up the vast majority of binaries and inclined circumbinary planets are dynamically allowable.

4.7. TOI 1897

TOI 1897 is an early G dwarf with an inferred RV semi-amplitude of $6.27^{+3.39}_{-1.15}$ km/s and a p-value less than 10^{-6} , placing it in the 100th percentile of excess RV noise of similar looking stars. A cursory examination of the SPOC light curve shows one transit too deep for a planetary object and sever of a smaller object. The probability of this system being an eclipsing binary where the primary transits have fallen into data gaps seems quite high.

4.8. TOI 4573

TOI 4573 is a late K dwarf with an inferred RV semi-amplitude of $5.39^{+1.90}_{-0.63}$ km/s and a p-value of less than 10^{-6} , placing it in the 100th percentile of excess RV noise of similar looking stars. The semi-amplitude inference is unusually confident because this source has been observed 78 times by Gaia RVs. This star is host to a $< 4R_{\oplus}$ planet in a to day orbit. Comments on the publicly available TRES follow-up spectra indicate the there is evidence of an RV trend in the system that is out-of-phase with the known transiting planet.

4.9. TOI 2119

TOI 2119 is an early dwarf with an inferred RV semi-amplitude of $13.15^{+7.11}_{-1.98}$ km/s and a p-value of 0 placing it in the 100th percentile of excess RV noise of similar looking stars. This star hosts a known eccentric brown dwarf companion (Carmichael et al. 2022; Cañas et al. 2022)

5. CONCLUSION

In this manuscript, we describe a statistical framework called **paired** for identifying stellar multiplicity using radial velocity information from Gaia EDR3. The resulting p-values are extracted from the three presently available measurements for a subset of Gaia target stars: the mean radial velocity, the error associated with the mean radial velocity, and number of radial velocity observations (or “transits”). From these values,

TIC	TOI	# of RV transits	K_{16th}	K_{50th}	K_{84th}	TFOP Disposition	Gaia m	T_{eff}
285048486	1728	29	1.041	1.369	1.909	CP	11.726	3907.0
468777766	3750	17	5.224	7.015	10.397	PC	13.958	3815.0
230387153	2086	34	3.538	4.318	5.957	PC	11.822	5337.0
468889418	5156	18	5.4	6.401	9.079	PC	10.67	5857.9
29960110	1201	3	1.23	2.78	8.538	CP	12.089	3948.0
322262448	4043	11	9.727	12.585	20.412	PC	12.702	5926.0
418012030	2533	27	9.669	11.438	16.342	PC	12.002	6144.3
236934937	2291	18	4.145	5.111	7.284	PC	12.946	3869.0
180695581	1807	15	2.344	2.85	4.189	CP	9.684	4612.99
236387002	2119	15	11.176	13.154	20.264	CP	11.486	3606.0
198212955	1242	8	2.247	3.352	5.785	PC	12.348	4255.0
372758077	4168	5	24.065	33.144	66.019	PC	11.865	6016.0
347013211	2045	10	8.885	10.974	18.528	PC	11.215	6125.9
374348168	4282	11	11.363	14.219	22.697	PC	12.525	5780.0
168405330	2984	19	42.72	50.967	73.418	PC	12.558	4935.8
362103298	4573	78	4.764	5.392	7.295	PC	11.802	4207.0
232608943	4600 ^a	18	4.633	5.968	8.593	PC	12.434	5073.0
366499151	5115	6	10.096	13.762	26.46	PC	12.651	5129.0
32497972	876	16	2.023	2.712	3.999	PC	12.477	3955.0
318812447	2634 ^a	5	2.13	3.776	8.023	PC	11.505	5349.16
163539739	1278	16	4.116	5.07	7.317	CP	12.74	3841.0
123664207	2493 ^a	46	1.674	2.092	2.892	PC	12.181	4242.0

^aSingle transit

Table 2. TESS planet hosts of particular interest

we construct a statistically robust mechanism for determining consistency between the reported radial velocity error for a source, and the distribution of radial velocity error for stars of similar color and magnitude. Where inconsistent, we generally assume that the excess noise is indicative of additional orbital reflex motion of the source (due to a companion). We demonstrate that this assumption is borne out in general when comparing to other benchmarks of binarity: samples of known eclipsing binaries, the clustering of “likely” binaries on the binary sequence of the HR diagram, and existing radial velocity catalogs. We include in this manuscript the resulting p -values reported by **paired** for the sample of Gaia radial velocity targets observed by NASA’s *Kepler* and *TESS* missions. This sample constitutes a sizeable fraction (9% and 15%, respectively) of all the stars in the *Kepler* Input Catalog and the *TESS* Community Target List.

There are, however, cases of “likely” binaries identified by **paired** that are *bona fide* single stars. These cases highlight the ways in which our results ought to be interpreted with caution. While meaningful in a statistical sense, the nature of **paired**’s

probabilistic diagnosis for an individual star merits careful consideration. Some fraction of the time (per the definition of the p -value), a star which we deem *likely* to exhibit excess RV noise does not do so. It may also be the case that the excess apparent RV noise is due to a physical mechanism other than reflex motion due to a companion. We focus on a key example here that highlights the necessity for caution.

TrES-2 (Kepler-1) was the the first star identified in the *Kepler* field to host a transiting planet, discovered from the ground several years prior to launch (O’Donovan et al. 2006). Its early discovery and subsequent high-precision photometry from *Kepler* render it a target of high interest, and it possesses a decade and a half of radial velocity observations. This star is a notable case for where archival RV data does not support the existence of the companion with a 50th-percentile semi-amplitude of ~ 5 km/s that is indicated in our catalog. Despite our advertised caution, this catalog is intended to be useful wherever some idea of the close binary rate of stars is useful. We have illustrated some possible uses for this catalog in constraining the binary fraction of planet hosts and identifying known planetary systems that have evidence for stellar or large sub-stellar companions. We are particularly interested in the prospect of using this catalog to particularize the suppression effect that close binaries have upon planet occurrence. We can see the suppression effect in the crude exercise of comparing the p -value distribution of known planet hosts to the field, but occurrence rate calculations demand a better understanding of possible false positive scenarios.

This work was performed in part through the Pre-Doctoral program at the Flatiron Institute’s Center for Computational Astrophysics.

Q. C.’s work was supported by the National Aeronautics and Space Administration under Grant No. 80NSSC21K1841 issued through the Future Investigators in NASA Earth and Space Science and Technology program.

This work has made use of data from the European Space Agency (ESA) mission *Gaia* (<https://www.cosmos.esa.int/gaia>), processed by the Gaia Data Processing and Analysis Consortium (DPAC; <https://www.cosmos.esa.int/web/gaia/dpac/consortium>). Funding for the DPAC has been provided by national institutions, in particular the institutions participating in the Gaia Multilateral Agreement.

This research has made use of the Exoplanet Followup Observation Program website (ExoFOP), which is operated by the California Institute of Technology, under contract with the National Aeronautics and Space Administration under the Exoplanet Exploration Program.

This research has made use of the NASA Exoplanet Archive, which is operated by the California Institute of Technology, under contract with the National Aeronautics and Space Administration under the Exoplanet Exploration Program.

This work made use of the *gaia-kepler.fun* crossmatch database created by Megan Bedell.

We are thankful for helpful discussions with Natalia Guerrero, Veselin Kostov, Kaitlin Kratter, Elisa Quintana, and Jamie Tayar.

Software: *astropy* (Astropy Collaboration et al. 2013, 2018), *numpy* (Harris et al. 2020), *matplotlib* (Hunter 2007), *pandas* (pandas development team 2020; Wes McKinney 2010), *numpyro* (Phan et al. 2019)

APPENDIX

A. MATHEMATICAL DETAILS OF THE MODEL

The next paper in this series (Foreman-Mackey, Chance, et al., in prep.) provides a more detailed description of our methodology, but we summarize the key elements here in order to provide some intuition for the procedure. For each RV target, the *Gaia* EDR3 catalog reports the median RV, an estimate of the error on this median, and the number of individual RV measurements (called “transits”) that were used in this estimate. In our analysis, we ignore the median RV and instead only consider the RV error and number of transits. The RV error ϵ_n for a target n is computed as (Katz et al. 2019)

$$\epsilon_n^2 = \left(\sqrt{\frac{\pi}{2T_n}} s_n \right)^2 + 0.11^2 \quad (\text{A1})$$

where

$$s_n^2 = \frac{1}{T_n - 1} \sum_{i=1}^{T_n} (v_{n,i} - \bar{v}_n)^2 \quad (\text{A2})$$

is the sample variance of the individual RV measurements $v_{n,t}$. In Equation A2, $t = 1, \dots, T_n$ indexes the T_n transits for target n and

$$\bar{v}_n = \frac{1}{T_n} \sum_{i=1}^{T_n} v_{n,i} \quad (\text{A3})$$

is the mean RV. In all that follows, it is much simpler to reason about the sample variance s_n^2 instead of the error on the median ϵ_n , but that isn't a problem because we can compute

$$s_n^2 = \frac{2T_n}{\pi} (\epsilon_n^2 - 0.11^2) \quad (\text{A4})$$

for any target, using only values available in the catalog: ϵ_n and T_n .

Now, for a given target n , in the absence of any excess radial velocity signal, and if we know it's per-transit radial velocity measurement uncertainty σ_n , we would expect the quantity

$$\xi_n^2 = \frac{(T_n - 1) s_n^2}{\sigma_n^2} \quad (\text{A5})$$

to be chi-squared distributed with $T_n - 1$ degrees of freedom.

We can even go one step further, and derive the expected sampling distribution for s_n^2 under some model for the excess RV signal. For example, in our case, we want to infer the orbital properties of any binary systems based on the observed s_n^2 . In this case, our model for the expected RV time series is

$$\mu_n(t; \theta_n) = v_{0,n} + K_n [\cos(f_n(t) + \omega_n) + e_n \cos \omega_n] \quad , \quad (\text{A6})$$

but the following derivation can be used more generally. We can evaluate Equation A6, at observation times $\{t_{n,i}\}_{i=1}^{T_n}$ and orbital parameters $\theta_n = \{K_n, e_n, \omega_n, \dots\}$. Of course, in our case, we don't actually *know* the observation times¹, so in practice we will need to marginalize those out, but for now, let's proceed as if we do know them. For a given set of parameters, it can be shown that the sampling distribution for our scalar

$$\xi_n^2 = \frac{(T_n - 1) s_n^2}{\sigma_n^2} \quad (\text{A7})$$

¹ The Gaia Observation Forecast Tool (<https://gaia.esac.esa.int/gost/>) predicts the transit times for astrometric measurements, and we expect the RV measurements will be a subset of these transits, but for most sources that information is not enough to substantially improve our inferences.

is a non-central χ^2 distribution with T_n degrees of freedom, and non-centrality parameter

$$\lambda = \sum_{i=1}^{T_n} \left[\frac{\mu_n(t_i; \theta_n) - \bar{\mu}_n}{\sigma_n} \right]^2 \quad (\text{A8})$$

where

$$\bar{\mu}_n = \frac{1}{T_n} \sum_{i=1}^{T_n} \mu_n(t_i; \theta_n) \quad (\text{A9})$$

is the sample mean of the model evaluated at the observation times. This sampling distribution defines a likelihood function for the parameters θ_n , and it is the key ingredient of our method.

A.1. *Per-transit radial velocity measurement uncertainty*

In the previous discussion, we assumed that the per-observation RV measurement uncertainty σ_n was known. This is not, however, a number that we have access to. Instead, we derive a hierarchical model for determining a calibrated data-driven estimate of σ_n , as a function of color and apparent magnitude, based on the published data. Across a coarse grid in color and apparent magnitude, we build a probabilistic model for the observed distribution of RV error in each bin using the non-central χ^2 likelihood defined by Equation A8 to allow for multiple star systems in the training set. This model is high dimensional—there is a parameter for each target in the bin!—so we use variational inference (e.g. Blei et al. 2017) as implemented by the `numpyro` software package (Phan et al. 2019) to make the model computationally tractable.

This procedure produces an estimate of the per-transit RV measurement uncertainty σ on a grid in color and apparent magnitude. We interpolate this grid to produce an estimate of the measurement uncertainty for each RV target in the *Gaia* catalog, and then use these results to compute p -values and semi-amplitudes for this sample.

REFERENCES

- | | |
|--|--|
| <p>Andrew, S., Penoyre, Z., Belokurov, V., Evans, N. W., & Oh, S. 2022, Binary parameters from astrometric and spectroscopic errors, and candidate massive dark companions in Gaia eDR3, arXiv, doi: 10.48550/ARXIV.2206.04392</p> <p>Astropy Collaboration, Robitaille, T. P., Tollerud, E. J., et al. 2013, <i>A&A</i>, 558, A33, doi: 10.1051/0004-6361/201322068</p> | <p>Astropy Collaboration, Price-Whelan, A. M., Sipőcz, B. M., et al. 2018, <i>AJ</i>, 156, 123, doi: 10.3847/1538-3881/aabc4f</p> <p>Blei, D. M., Kucukelbir, A., & McAuliffe, J. D. 2017, <i>Journal of the American statistical Association</i>, 112, 859</p> <p>Carmichael, T. W., Irwin, J. M., Murgas, F., et al. 2022, arXiv:2202.08842 [astro-ph]. http://arxiv.org/abs/2202.08842</p> |
|--|--|

- Cañas, C. I., Mahadevan, S., Bender, C. F., et al. 2022, *The Astronomical Journal*, 163, 89, doi: [10.3847/1538-3881/ac415f](https://doi.org/10.3847/1538-3881/ac415f)
- Chen, Z., & Kipping, D. 2021, arXiv e-prints, arXiv:2112.00966. <https://arxiv.org/abs/2112.00966>
- Chontos, A., Murphy, J. M. A., MacDougall, M. G., et al. 2022, *The Astronomical Journal*, 163, 297
- Ciardi, D. R., Beichman, C. A., Horch, E. P., & Howell, S. B. 2015, *ApJ*, 805, 16, doi: [10.1088/0004-637X/805/1/16](https://doi.org/10.1088/0004-637X/805/1/16)
- Clark, B. M., Blake, C. H., & Knapp, G. R. 2011, *The Astrophysical Journal*, 744, 119, doi: [10.1088/0004-637x/744/2/119](https://doi.org/10.1088/0004-637x/744/2/119)
- Coughlin, J. L., Mullally, F., Thompson, S. E., et al. 2016, *ApJS*, 224, 12, doi: [10.3847/0067-0049/224/1/12](https://doi.org/10.3847/0067-0049/224/1/12)
- Czekala, I., Chiang, E., Andrews, S. M., et al. 2019, *ApJ*, 883, 22, doi: [10.3847/1538-4357/ab287b](https://doi.org/10.3847/1538-4357/ab287b)
- Duquenois, A., & Mayor, M. 1991, *A&A*, 248, 485
- El-Badry, K., Rix, H.-W., & Heintz, T. M. 2021, *Monthly Notices of the Royal Astronomical Society*, 506, 2269, doi: [10.1093/mnras/stab323](https://doi.org/10.1093/mnras/stab323)
- Fischer, D. A., & Valenti, J. 2005, *The Astrophysical Journal*, 622, 1102, doi: [10.1086/428383](https://doi.org/10.1086/428383)
- Foreman-Mackey, D., Morton, T. D., Hogg, D. W., Agol, E., & Schölkopf, B. 2016, *The Astronomical Journal*, 152, 206, doi: [10.3847/0004-6256/152/6/206](https://doi.org/10.3847/0004-6256/152/6/206)
- Gajdoš, P., Parimucha, Š., Hambálek, Ľ., & Vaňko, M. 2017, *MNRAS*, 469, 2907, doi: [10.1093/mnras/stx963](https://doi.org/10.1093/mnras/stx963)
- Guerrero, N. M. 2021, *The Astrophysical Journal Supplement Series*, 29
- Harris, C. R., Millman, K. J., van der Walt, S. J., et al. 2020, *Nature*, 585, 357, doi: [10.1038/s41586-020-2649-2](https://doi.org/10.1038/s41586-020-2649-2)
- Holman, M. J., & Wiegert, P. A. 1999, *The Astronomical Journal*, 117, 621, doi: [10.1086/300695](https://doi.org/10.1086/300695)
- Hunter, J. D. 2007, *Computing in Science & Engineering*, 9, 90, doi: [10.1109/MCSE.2007.55](https://doi.org/10.1109/MCSE.2007.55)
- Katz, D., Sartoretti, P., Cropper, M., et al. 2019, *A&A*, 622, A205, doi: [10.1051/0004-6361/201833273](https://doi.org/10.1051/0004-6361/201833273)
- Kirk, B., Conroy, K., Prša, A., et al. 2016, *AJ*, 151, 68, doi: [10.3847/0004-6256/151/3/68](https://doi.org/10.3847/0004-6256/151/3/68)
- Knutson, H. A., Fulton, B. J., Montet, B. T., et al. 2014, *The Astrophysical Journal*, 785, 126, doi: [10.1088/0004-637X/785/2/126](https://doi.org/10.1088/0004-637X/785/2/126)
- Kostov, V. B., Orosz, J. A., Feinstein, A. D., et al. 2020, *AJ*, 159, 253, doi: [10.3847/1538-3881/ab8a48](https://doi.org/10.3847/1538-3881/ab8a48)
- Kraus, A. L., Ireland, M. J., Hillenbrand, L. A., & Martinache, F. 2012, *The Astrophysical Journal*, 745, 19, doi: [10.1088/0004-637X/745/1/19](https://doi.org/10.1088/0004-637X/745/1/19)
- Kraus, A. L., Ireland, M. J., Huber, D., Mann, A. W., & Dupuy, T. J. 2016, *AJ*, 152, 8, doi: [10.3847/0004-6256/152/1/8](https://doi.org/10.3847/0004-6256/152/1/8)
- Kunimoto, M., Daylan, T., Guerrero, N., et al. 2022, *ApJS*, 259, 33, doi: [10.3847/1538-4365/ac5688](https://doi.org/10.3847/1538-4365/ac5688)
- Lissauer, J. J., Marcy, G. W., Bryson, S. T., et al. 2014, *ApJ*, 784, 44, doi: [10.1088/0004-637X/784/1/44](https://doi.org/10.1088/0004-637X/784/1/44)
- Maoz, D., Badenes, C., & Bickerton, S. J. 2012, *The Astrophysical Journal*, 751, 143, doi: [10.1088/0004-637x/751/2/143](https://doi.org/10.1088/0004-637x/751/2/143)
- Martin, D. V., & Triaud, A. H. M. J. 2014, *Astronomy & Astrophysics*, 570, A91, doi: [10.1051/0004-6361/201323112](https://doi.org/10.1051/0004-6361/201323112)
- Martin, R. G., & Lubow, S. H. 2017, *The Astrophysical Journal*, 835, L28, doi: [10.3847/2041-8213/835/2/L28](https://doi.org/10.3847/2041-8213/835/2/L28)
- Marzari, F., & Gallina, G. 2016, *Astronomy & Astrophysics*, 594, A89, doi: [10.1051/0004-6361/201628342](https://doi.org/10.1051/0004-6361/201628342)
- Maxted, P. F. L., & Jeffries, R. D. 2005, *MNRAS*, 362, L45, doi: [10.1111/j.1745-3933.2005.00073.x](https://doi.org/10.1111/j.1745-3933.2005.00073.x)
- Moe, M., & Kratter, K. M. 2021, *Monthly Notices of the Royal Astronomical Society*, 507, 3593, doi: [10.1093/mnras/stab2328](https://doi.org/10.1093/mnras/stab2328)
- Ngo, H., Knutson, H. A., Hinkley, S., et al. 2015, *The Astrophysical Journal*, 800, 138, doi: [10.1088/0004-637X/800/2/138](https://doi.org/10.1088/0004-637X/800/2/138)

- O'Donovan, F. T., Charbonneau, D., Mandushev, G., et al. 2006, *ApJL*, 651, L61, doi: [10.1086/509123](https://doi.org/10.1086/509123)
- Offner, S. S. R., Moe, M., Kratter, K. M., et al. 2022, arXiv:2203.10066 [astro-ph]. <http://arxiv.org/abs/2203.10066>
- Paardekooper, S.-J., Thébault, P., & Mellema, G. 2008, *Monthly Notices of the Royal Astronomical Society*, 386, 973, doi: [10.1111/j.1365-2966.2008.13080.x](https://doi.org/10.1111/j.1365-2966.2008.13080.x)
- pandas development team, T. 2020, pandas-dev/pandas: Pandas, latest, Zenodo, doi: [10.5281/zenodo.3509134](https://doi.org/10.5281/zenodo.3509134)
- Penoyre, Z., Belokurov, V., & Evans, N. W. 2022a, *Monthly Notices of the Royal Astronomical Society*, 513, 2437, doi: [10.1093/mnras/stac959](https://doi.org/10.1093/mnras/stac959)
- . 2022b, *Monthly Notices of the Royal Astronomical Society*, doi: [10.1093/mnras/stac1147](https://doi.org/10.1093/mnras/stac1147)
- Phan, D., Pradhan, N., & Jankowiak, M. 2019, arXiv e-prints, arXiv:1912.11554. <https://arxiv.org/abs/1912.11554>
- Piskorz, D., Knutson, H. A., Ngo, H., et al. 2015, *The Astrophysical Journal*, 814, 148, doi: [10.1088/0004-637X/814/2/148](https://doi.org/10.1088/0004-637X/814/2/148)
- Pourbaix, D., Tokovinin, A. A., Batten, A. H., et al. 2009, *VizieR Online Data Catalog*, B/sb9
- Price-Whelan, A. M., Hogg, D. W., Foreman-Mackey, D., & Rix, H.-W. 2017, *The Astrophysical Journal*, 837, 20
- Price-Whelan, A. M., Hogg, D. W., Foreman-Mackey, D., & Rix, H.-W. 2017, *ApJ*, 837, 20, doi: [10.3847/1538-4357/aa5e50](https://doi.org/10.3847/1538-4357/aa5e50)
- Price-Whelan, A. M., Hogg, D. W., Rix, H.-W., et al. 2020, *The Astrophysical Journal*, 895, 2, doi: [10.3847/1538-4357/ab8acc](https://doi.org/10.3847/1538-4357/ab8acc)
- Prša, A., Kochoska, A., Conroy, K. E., et al. 2022, *ApJS*, 258, 16, doi: [10.3847/1538-4365/ac324a](https://doi.org/10.3847/1538-4365/ac324a)
- Silsbee, K., & Rafikov, R. R. 2015, *ApJ*, 798, 71, doi: [10.1088/0004-637X/798/2/71](https://doi.org/10.1088/0004-637X/798/2/71)
- Stassun, K. G., Oelkers, R. J., Paegert, M., et al. 2019, *AJ*, 158, 138, doi: [10.3847/1538-3881/ab3467](https://doi.org/10.3847/1538-3881/ab3467)
- Su, X.-N., Xie, J.-W., Zhou, J.-L., & Thebault, P. 2021, *The Astronomical Journal*, 162, 272, doi: [10.3847/1538-3881/ac2ba3](https://doi.org/10.3847/1538-3881/ac2ba3)
- Sun, L., Ioannidis, P., Gu, S., et al. 2019, *Astronomy & Astrophysics*, 624, A15, doi: [10.1051/0004-6361/201834275](https://doi.org/10.1051/0004-6361/201834275)
- Teske, J., Wang, S. X., Wolfgang, A., et al. 2021, *The Astrophysical Journal Supplement Series*, 256, 33
- Uehara, S., Kawahara, H., Masuda, K., Yamada, S., & Aizawa, M. 2016, *The Astrophysical Journal*, 822, 2, doi: [10.3847/0004-637X/822/1/2](https://doi.org/10.3847/0004-637X/822/1/2)
- Wang, J., Fischer, D. A., Xie, J.-W., & Ciardi, D. R. 2014, *The Astrophysical Journal*, 791, 111, doi: [10.1088/0004-637X/791/2/111](https://doi.org/10.1088/0004-637X/791/2/111)
- Wang, J., Fischer, D. A., Barclay, T., et al. 2015, *The Astrophysical Journal*, 815, 127, doi: [10.1088/0004-637X/815/2/127](https://doi.org/10.1088/0004-637X/815/2/127)
- Wes McKinney. 2010, in *Proceedings of the 9th Python in Science Conference*, ed. Stéfan van der Walt & Jarrod Millman, 56 – 61, doi: [10.25080/Majora-92bf1922-00a](https://doi.org/10.25080/Majora-92bf1922-00a)
- Wood, M. L., Mann, A. W., & Kraus, A. L. 2021, *The Astronomical Journal*, 162, 128, doi: [10.3847/1538-3881/ac0ae9](https://doi.org/10.3847/1538-3881/ac0ae9)
- Ziegler, C., Tokovinin, A., Latiolais, M., et al. 2021, *The Astronomical Journal*, 162, 192, doi: [10.3847/1538-3881/ac17f6](https://doi.org/10.3847/1538-3881/ac17f6)
- Ziegler, C., Law, N. M., Baranec, C., et al. 2018, *AJ*, 155, 161, doi: [10.3847/1538-3881/aab042](https://doi.org/10.3847/1538-3881/aab042)